Experimental study of the size effect on transverse cracking in cross-ply laminates and comparison with the main theoretical models

I.G. García[a], J. Justo[a], A. Simon[a,b], V. Mantič[a]

[a] *Grupo de Elasticidad y Resistencia de Materiales, Escuela Tcnica Superior de Ingeniería, Universidad de Sevilla Camino de los Descubrimienos s/n, 41092 Sevilla, Spain*
[b] *Keolis Lille, 276 Avenue de la Marne, 59700 Marcq en Baroeul, France*

Abstract

Transverse cracking of off-axis plies is typically the first step of some failure mechanisms in long fiber reinforced laminated composites. It is well known that the off-axis ply thickness affects strongly the strain level which this ply is able to withstand without cracking. Experimental evidences show that this critical strain level increases strongly with decreasing ply thickness for the thinnest plies, confirming a clear size effect. This fact could be used to inhibit transverse cracking with the use of the recently developed ultra-thin plies. However the classical failure criteria for composites are not able to predict this size effect. From the first tests in the 1970s, several models with very different hypotheses were proposed to predict this size effect. Surprisingly there is still not a clear consensus in the scientific community about which is the adequate model, though their fundamentals are radically different. In this work an extensive test campaign is carried out on self-similar $[0/90]_s$ cross-ply laminates of AS4/8552 carbon/epoxy. The size effect is evaluated spanning a broader spectrum of thicknesses than in the tests presented in the literature until now, in order to explore the range of thicknesses where the differences between predictions of the main theoretical models are larger. In spite of the inherent dispersion in the experimental results, the comparison shows that the purely stress-based criteria underestimates the apparent strength of the off-axis ply. The other models predict very similar results, particularly for the thinnest laminates, with slight underestimations or overestimations, depending on the model.

Keywords: trasnverse cracking, size effect, ultra-thin plies, in-situ strength

1. Introduction

The use of composites is extended across a wide range of structural applications. These materials are applied even in primary parts of structures in industries where lightweight is a key aspect. Despite this fact, the main failure mechanisms are not totally understood, as has been shown in the different world-wide failure exercises organized, see e.g. Hinton et al. (2004); Hinton and Kaddour (2013). This fact also explains the diversity of failure criteria which are currently used in the industry. The lack of a complete knowledge about the failure mechanisms causes conservative designs, including high safety factors (without certainty about the actual reserve of strength) and the overuse of already tested configurations.

The main reason for the uncertainty about the failure criteria is the inherent complexity of the micro- and meso-structure of composites, which affects the development and interactions of different failure mechanisms. How failures begin at the micro-scale, how they progress to become cracks at the meso-scale and how the micro-structure affects these steps are still an open issue. A huge effort has been carried out to relate these failure mechanisms, see e.g. Wang (1984); Schultheisz and Waas (1996); Landis et al. (2000); París et al. (2003); Tay et al. (2008). The key aspects of these studies is the use of fracture or damage mechanics to understand the failure development at different scales.

Transverse cracking is one of the most controversial failure mechanisms in composites. The term transverse cracking refers to the appearance of matrix cracks spanning the majority of the ply-thickness in off-axis plies. This is the first step of some failure mechanisms, inducing e.g. the appearance of delamination, see Berthelot

Email address: israelgarcia@us.es (I.G. García)

(2003), or oblique cracks, see Parvizi and Bailey (1978); Jalalvand et al. (2014). The most simple problem, but representative of the complex behavior, is the transverse cracking in cross-ply laminates subjected to tension. The most surprising experimental result is that the onset of transverse cracking does not depend exclusively of the stress or strain level in the off-axis ply where the crack onset occur, but it also depends on the thickness of the off-axis ply, see Parvizi and Bailey (1978). They found that the apparent strength is higher when the off-axis ply is thinner. The size effect found is in total disagreement with the failure criteria typically used in the industry as Maximum Strain, Maximum Stress, Hill-Tsai, Tsai-Wu or Hashin, see Sun et al. (1996); París (2001) for reviews. However, predicting this size effect is relevant given the recent development and usage of ultra-thin plies to increase the apparent strength of the off-axis plies. After the publications of a series of related experiments in 1970's (see below) many models have been proposed to explain this size effect which were based on very different fundamental hypotheses about how cracks initiate at different scales. These models will be revisited, analyzed and expressed in a common framework in Section 2.

First experiments reporting the influence of the off-axis ply thickness on its strength are due to Garrett and Bailey (1977) in the context of experiments in $[0/90_n]_s$ cross-ply specimens made from glass/epoxy with other objective: the evaluation of the difference between the transverse strength and matrix strength. More specifically with the objective of evaluating the size effect, Parvizi et al. (1978) presented some experiments with glass/epoxy cross-ply laminates showing clearly the presence of a size effect and even finding the total constraining of the transverse cracking below a certain thickness of the off-axis ply. Subsequently, Parvizi and Bailey (1978) published experimental results about the accumulation of transverse cracks and the evolution of the crack density with the external load, which was followed by a large amount of works studying the crack density, see Nairn (2000) for a review. Focusing on the experimental works which deal with the first crack onsets, some interesting result were presented later: Boniface et al. (1997) carried out experiments to evaluate if the crack initiation is flaw sensitive by testing laminates with and without pre-induced defects. They found that for thin laminates the failure was not sensitive to defects, whereas they did observed an influence of the defects on the failure progress for thick laminates. Smith et al. (1998) evaluated experimentally the difference between $[0/90]_s$ and $[90, 0]_s$ carbon/epoxy laminates finding that the apparent strength is lower when the off-axis plies are the outer plies. Okabe et al. (2004) carried out experiments on current glass/epoxy cross-ply laminates and found a moderate dispersion between the results for the same coupon thicknesses but confirmed this size effect for current glass/epoxy cross-ply laminates. The influence of the damage previous to the loading was studied experimentally by Nouri et al. (2013) finding a strong interaction between the two. Recently Okabe et al. (2015) observed experimentally that the first transverse cracks begin at the micro-scale level at the free-edge.

This work presents the results of a new set of experiments carried out over a composite currently used in the industry, with self-similar laminates spanning a wide range of thicknesses and a large number of specimens per value of thickness. The objective of this work is to confirm the size effect for modern composites and analyse the prediction capability of the different theoretical models by comparing with new experimental results. The laminates under study will be cross-ply laminates $[0_n/90_n/0_n]$ with n being the number of plies of the same orientation which are placed together.

This article is organized as follows: the main theoretical models are reviewed and discussed in Section 2. The design, configuration and fabrication of the test specimens is described in Section 3. The testing procedure and the main findings during the experiments are discussed in Section 4. Finally the experimental results and their comparison with the theoretical models are presented in Section 5.

2. Theoretical models

This section describes the main theoretical models presented in the literature to explain and predict the size effect found in the transverse cracking of cross-ply laminates. The presentation of the models in the literature combines typically some fundamental hypotheses about how cracks initiate along with some procedures to approximate the necessary elastic and fracture results as stresses, energy release rate or released energy. Based on this combination, different authors introduced mathematical expressions to predict the critical value of the control parameters leading to the first transverse crack onsets. This section focuses on discussing the fundamental hypotheses of different models. Instead of using the original expressions based on different approximations of the required elastic and fracture results, this section develops new expressions based on the original hypotheses of each model but combined with a common framework providing more accurate approximations

of the elastic and fracture results necessary for each model. In this way the inaccuracies introduced by the different approximations traditionally used for each model do not affect the present comparison.

In accordance with the experiments presented later, the application of theoretical models will be based on the assumption that the laminates are subjected to tension in the direction of the outer-ply fibers. For the sake of coherence in the presentation of the models, the loading direction is identified with the y-axis while for each ply the usual notation in composites is used: 1-axis is the fiber direction, and 2- and 3-axes correspond to the in-plane and out-of-plane transverse directions respectively. Since the experimental results will measure the critical value of the mechanical strain imposed by the testing machine for which the first crack onset occur, in the analysis of each model the expression to predict the transverse cracking will be expressed in terms of a critical value of the longitudinal strain $\varepsilon^{\mathrm{c}}_{yy}$. The different theoretical models are discussed from Section 2.1 to Section 2.5, whereas Section 2.6 describes a common framework to include the residual thermal stresses in these theoretical models.

2.1. Models based on stress criteria

The models based on stress criteria were the first employed to predict failure in composites, see e.g. Vasil'ev et al. (1970); Garrett and Bailey (1977). They assume the existence of critical values for stresses in each ply and direction. Once the stresses in a certain ply reach a critical value, a failure occurs in this ply. These critical values are considered as material properties. Thus, the stresses are obtained using an elastic analysis and are compared with the critical values for each ply and direction. In the particular case of a transverse ply, the parameter governing the failure studied here is the transverse strength Y_{t}, which is the critical value for the transverse longitudinal stresses $\sigma^{(90)}_{yy}$. Thus, according to this model, the first crack onset occur when

$$\sigma^{(90)}_{yy} = Y_{\mathrm{t}} \tag{1}$$

Using the laminate theory, $\sigma^{(90)}_{yy}$ can be estimated as a function of the transverse strain ε_{yy}. With this expression the critical strain promoting the first transverse crack onset $\varepsilon^{\mathrm{c}}_{yy}$ is given by the following expression:

$$\varepsilon^{\mathrm{c}}_{yy} = \frac{Y_{\mathrm{t}}}{\tilde{E}_{22}}, \tag{2}$$

with

$$\tilde{E}_{22} = \frac{1-\nu_{12}\nu_{21}\frac{1+\frac{t_0}{t_{90}}}{1+\frac{E_{22}}{E_{11}}\frac{t_0}{t_{90}}}}{1-\nu_{12}\nu_{21}} E_{22} \tag{3}$$

deduced in García et al. (2014) where t_0 and t_{90} are the outer- and inner-ply thicknesses, see Figure 1. The terms, E_{11}, E_{22} refer to the longitudinal and transverse elastic moduli, and ν_{12} and ν_{21} refer to Poisson's ratios, where 1 and 2 define fiber and transverse directions in a unidirectional ply. The expression presented here for failure in a transverse ply in a cross-ply laminate is common for the majority of the classic stress-based failure criteria as Maximum Strain, Maximum Stress, Tsai-Hill, Tsai-Wu or Hashin.

The most attractive feature of these criteria is the simplicity in their application. In the majority of cases they are based on exclusively linear elastic analysis to obtain the stress state in each ply composing the laminate. Once the stress state is known, the stresses are compared at the ply level with the critical values. Thus, the influence of the neighboring plies on the failure behavior of each ply is neglected. Although this is an extremely simplifying hypothesis in view of the experimental evidences, the typical errors remain on the conservative side.

The main weak point of these criteria is that they are not able to explain the size effect observed in the experiments. The expression in (2) depends very weakly on the ratio t_0/t_{90}, while it is independent of any dimensional geometric parameter, therefore the expression is scale-independent.

2.2. Model based on inherent flaw mechanics

This model, initially proposed by Dvorak and Laws (1985, 1986, 1987), is mainly based on assuming the existence of a critical crack length δ_{c} that determines which law governs the crack growth. According to Dvorak and Laws (1987), below this critical length the transverse cracks grow in a stable and time-dependent manner (also referred to as flaws or "non-Griffith cracks") in spite of the unstable growth that a classical fracture

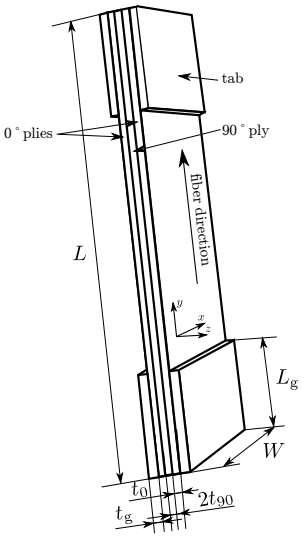

n_{90°	L (mm)	W (mm)	$2t_{90}$ (mm)	t_0 (mm)	L_g (mm)	t_g (mm)
1	160	25	0.19	0.19	37	1.6
2	160	25	0.38	0.38	37	1.6
3	160	25	0.57	0.57	37	1.6
4	160	25	0.76	0.76	37	1.6
5	160	25	0.95	0.95	40	1.6
7	160	25	1.33	1.33	48	1.6
10	160	25	1.90	1.90	48	1.6
16	160	25	3.04	3.04	56	1.6

Figure 1: Geometrical description of the specimen tested.

mechanics analysis would predict. Once the cracks reach the critical length, their growth becomes governed by the classical Griffith criterion. Then, the crack growth can be predicted by the typical balance between the energy release rate $G(a)$ when the crack length reaches the critical length $a = \delta_c$ and the transverse fracture toughness G_c: $G(\delta_c) \geq G_c(\delta_c)$.

The critical length δ_c is considered a material property which depends strongly on the material microstructure at the fiber scale. The reason for this consideration is that the first step of stable crack growth is justified by the presence of impediments to the crack growth at the fiber scale. With basis on the existence of this critical length, the fracture behavior is very different if the critical length is either shorter or longer than the transverse-ply thickness $2t_{90}$. If $\delta_c \ll t_{90}$ (thick plies) the unstable crack growth occurs along the direction perpendicular to the interface, i.e. through the thickness, because the crack length reaches δ_c before spanning the whole thickness. By contrast, if $\delta_c \gg t_{90}$ (thin plies), the crack reaches the interface before being governed by the classical Griffith criterion. In this case the unstable crack growth occurs in the direction parallel to the fibers of the transverse ply as a tunneling crack, i.e. through the width. When $\delta_c \approx t_{90}$ an intermediate behavior is predicted.

The form of the energy release rate $G(a)$ is very different for a crack growing through the thickness and through the width, see Dvorak and Laws (1987); Ho and Suo (1993). Whereas $G_t(a)$ for a crack growth through the thickness increases with a, except very near the interface where it vanishes quickly, see Blázquez et al. (2008), the value of $G_l(a)$ for a crack growing through the width tends asymptotically to a constant value, see Ho and Suo (1993). This fact leads to a very different trends in the size effect for thin and thick laminates. The critical strain ε^c_{yy} is given by the following expression,

$$\varepsilon^c_{yy} = \begin{cases} \sqrt{\dfrac{G_{ct}}{E_{22} t_{90} \hat{G}_t(\delta_c/t_{90})}}, & \text{if } \delta_c \ll t_{90} \\ \sqrt{\dfrac{G_{cl}}{E_{22} t_{90} \hat{G}_l(\delta_c/t_{90})}}, & \text{if } \delta_c \gg t_{90} \end{cases} \tag{4}$$

where G_{ct} and G_{cl} are the transverse fracture toughness when the crack grows through the thickness and the width, respectively. In the intermediate case for $\delta_c \sim t_{90}$ an unstable crack growth is found when $G_t = G_{ct}$. The terms $\hat{G}_t$ and $\hat{G}_l$ denote the dimensionless energy release rates,

$$\hat{G}_{(\cdot)}(a/t_{90}) = \frac{G_{(\cdot)}(a)}{E_{22}\varepsilon^2_{yy} t_{90}} \tag{5}$$

where a is the crack length in the thickness direction and the subindex t and l refer to the transverse and longitudinal direction.

The application of this model has been typically associated to the approximation of the energy release rates G using shear-lag methods or other simplifying methods. This is a good strategy to easily provide expressions to be applied in an engineering context. However, the objective here is to compare different models focusing on their assumptions. Thus, the energy release rate is approximated here using very accurate solutions presented by Blázquez et al. (2008) and computed by the Boundary Element Method (BEM), with results detailed in Appendix B.

Due to its nature, the critical length δ_{c} is very difficult to measure. For this reason δ_{c} is obtained typically in an indirect form. Assuming that the main idea of the model can be applied to a unidirectional laminate subjected to a uniaxial transverse load, the transverse strength is given by a crack reaching the critical length δ_{c} when growing from the free edge. Thus, δ_{c} can be expressed as a combination of the unidirectional critical transverse strain $Y_{\varepsilon \mathrm{t}} = Y_{\mathrm{t}}/E_{22}$ and G_{ct},

$$\delta_{\mathrm{c}} = \frac{G_{\mathrm{ct}} E_{22}}{1.12^2 \pi Y_{\mathrm{t}}^2} \tag{6}$$

where the value 1.12^2 derives from the factor for the stress intensity factor of a crack growing in a semi-infinite plane from the free edge with respect to a crack in an infinite plane[1].

Once δ_{c} is obtained, the critical strain $\varepsilon_{yy}^{\mathrm{c}}$ can be predicted by the following expression:

$$\varepsilon_{yy}^{\mathrm{c}} = \begin{cases} 1.12 Y_{\varepsilon \mathrm{t}}, & \text{if } \delta_c \ll t_{90} \text{ (thick laminates)}, \\ \sqrt{\frac{G_{\mathrm{c}}}{E_{22} t_{90}} \frac{1}{\hat{G}_{\mathrm{t}}(\delta_{\mathrm{c}}/t_{90})}}, & \text{if } \delta_c \lesssim t_{90} \text{ (mid-thickness laminates)}, \\ \sqrt{\frac{G_{\mathrm{c}}}{E_{22} t_{90}} \frac{1}{\int_0^1 \hat{G}_{\mathrm{t}}(\hat{a}) \mathrm{d}\hat{a}}}, & \text{if } \delta_c \gg t_{90} \text{ (thin laminates)}, \end{cases} \tag{7}$$

where the asymptotic behavior for $\hat{G}_{\mathrm{t}}$ and $\hat{G}_{\mathrm{l}}$, discussed by, e.g., Ho and Suo (1993); García et al. (2014), has been assumed for $\delta_c \ll t_{90}$ and $\delta_c \gg t_{90}$. In addition, the hypothesis of $G_{\mathrm{ct}} = G_{\mathrm{cl}} = G_{\mathrm{c}}$ has been assumed following the works using this model, due to the lack of experimental evidences of a significant difference between values of G_{ct} and G_{cl}.

The key idea behind this model has been used and extended by many authors from the publication of the seminal article by Dvorak and Laws (1985), see a recent review by van der Meer and Dávila (2013). Previously to the works by Dvorak and Laws (1985, 1986, 1987), several authors proposed the same idea with the difference of restricting the flaw growth to occur through the thickness (Wang and Crossman, 1980; Wang et al., 1985). More recently Camanho et al. (2006) presented a nonlinear correction for the expressions provided by Dvorak and Laws (1987) for in-plane shear loading due to a strongly nonlinear behavior observed for this type of loading. In addition this model has been implemented in a general constitutive damage model for the ply (Maimí et al., 2007). Some of these works assume the pre-existence of a crack with length δ_{c} instead of assuming a previous flaw which grows stably up to reaching the critical length. In terms of the predicted critical strain $\varepsilon_{yy}^{\mathrm{c}}$ these two hypotheses are totally equivalent.

Figure 2 shows the critical transverse strain $\varepsilon_{yy}^{\mathrm{c}}$ predicted by this model as a function of the inner-ply thickness $2t_{90}$ for a cross-ply laminate $[0_n/90_{n/2}]_{\mathrm{s}}$ of carbon/epoxy with properties detailed in Table 1. For thin laminates, see (7), the critical strain $\varepsilon_{yy}^{\mathrm{c}}$ increases when the transverse-ply thickness t_{90} is reduced. In addition, for thick laminates the critical strain is not given by the unidirectional critical transverse strain $Y_{\varepsilon \mathrm{t}}$ but for a value which is 1.12 times this property $Y_{\varepsilon \mathrm{t}}$. This result has motivated the concept of "in-situ strength" for plies inside a laminate in contrast to the strength of unidirectional laminates, see Flaggs and Kural (1982); Chang and Chen (1987). This concept is extensively used to denote this difference independently of the laminate thickness and the model used.

The main weak point of this model is the hypothesis about the existence of a critical length δ_{c} which is a material property. The changing-behavior from a stable to an unstable growth as a function of the flaw or crack length needs to be justified, likely at the micromechanical level. A very interesting attempt has been presented by van der Meer and Dávila (2013) using a cohesive zone model in a mesoscopic model. Similarly, the alternative hypothesis of the pre-existence of a crack with a length which is a material property should be verified experimentally.

[1] Note that this result is obtained for isotropic materials. This model uses this result by assuming that the ply can be considered as transversely isotropic in the plane transverse to the fiber direction.

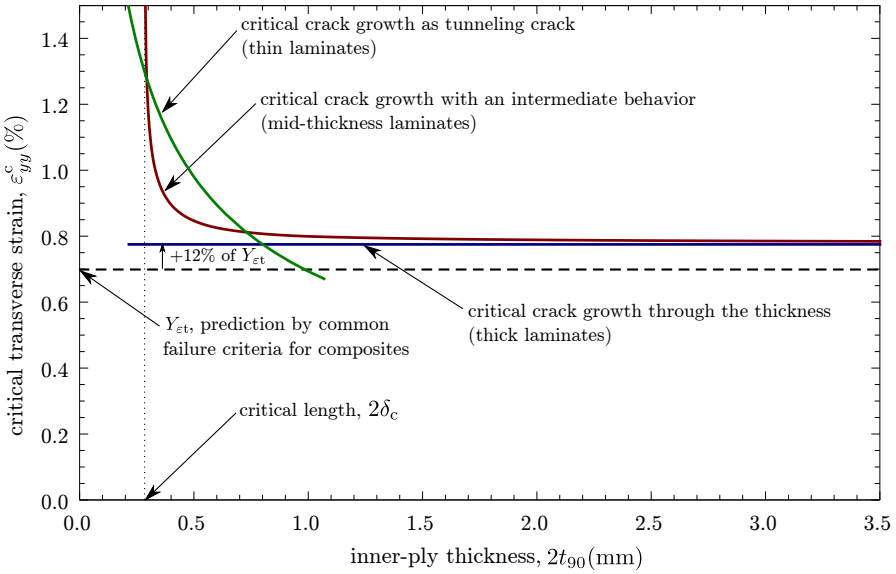

Figure 2: Model based on inherent flaw mechanics, Dvorak and Laws (1986). Prediction of the critical transverse strain as a function of the inner-ply thickness for cross-ply laminates $[0_n/90_{n/2}]_s$ of AS4/8852 carbon/epoxy with properties in Table 1.

2.3. Model based on incremental energy criteria

This model is based on the hypothesis that a transverse crack onset with a certain finite length occurs when an energetic condition is fulfilled. The condition for a crack onset is given by the application of the First law of Thermodynamics to the energetic balance between the states before and after an abrupt crack onset. The intermediate states are neglected in the analysis assuming that they occur at a much smaller time scale. Then, neglecting heat exchange, this condition takes the form

$$\Delta\Pi + \Delta E_k + \Delta\Gamma = 0 \tag{8}$$

where $\Delta\Pi$ and ΔE_k are the increment in potential elastic and kinetic energy, respectively. The term $\Delta\Gamma$ denotes the dissipated energy in irreversible processes during the crack onset.

The incremental energy criterion, also denoted Finite Fracture Mechanics (FFM) by Hashin (1996) and collaborators, has been intermittently proposed in the literature, Aveston et al. (1971) applied it to other problem, while Garrett and Bailey (1977); Hashin (1996) applied it to the present problem. In the majority of applications the selection of the crack length after the onset is associated to the problem. In the case of cross-ply laminates, the crack is assumed to span the entire width and thickness of the transverse ply immediately after the onset (Garrett and Bailey, 1977; Hashin, 1996; Nairn, 2000). Under this hypothesis, the energetic condition (8) for a crack onset can be written as,

$$\varepsilon^c_{yy} = \sqrt{\frac{G_c}{E_{22}t_{90}}\frac{1}{\int_0^1 \hat{G}(a'/t_{90})\mathrm{d}(a'/t_{90})}} \tag{9}$$

where a quasi-static state has been assumed immediately before the crack onset (it implies $\Delta E_k \geq 0$). The dissipated energy $\Delta\Gamma$ is approximated by the multiplication of the fracture toughness G_c and the crack area. The change in potential elastic energy $\Delta\Pi$ is calculated by integrating the energy release rate G between the states before and after the crack onset. The dimensionless form of G used previously (5) has been employed. Different applications of this criterion to the present problem has been associated to more or less accurate methods for estimating $\Delta\Pi$, as different shear-lag strategies Garrett and Bailey (1977); Parvizi et al. (1978) or variational techniques (Hashin, 1996; Nairn, 2000). In the present work, $\Delta\Pi$ is evaluated using a very accurate numerical solution for $\hat{G}$ to avoid differences between the models based on distinct approximations.

Figure 3 shows the critical transverse strain ε^c_{yy} predicted by this model as a function of the inner-ply thickness $2t_{90}$. For thin laminates the size effect predicted is exactly the same as for the model based on the

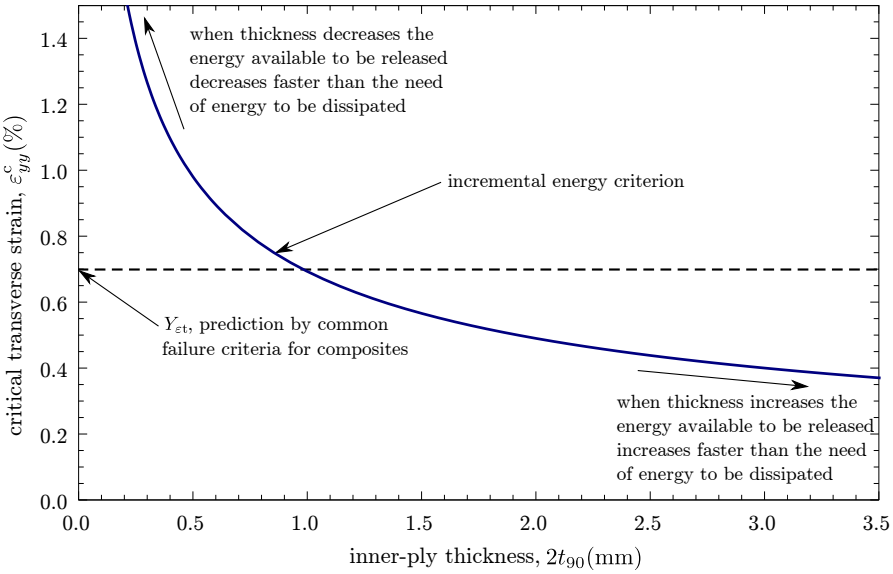

Figure 3: Model based on an incremental energy criterion, Hashin (1996). Prediction of the critical transverse strain as a function of the inner-ply thickness for cross-ply laminates $[0_n/90_{n/2}]_s$ of AS4/8552 carbon/epoxy with properties in Table 1.

inherent flaw mechanics. However, the cause given for this size effect is very different in the incremental energy criterion from the inherent flaw mechanics. For the energy criterion, the cause of the size effect is the geometric dissimilarity between the scales of the geometric entities where the energy is released and dissipated. The potential elastic energy is released in a bulk whereas the energy is dissipated at the new crack surface. As a consequence, if the laminate thickness is reduced for a fixed strain level, both the required dissipated energy and the available potential elastic energy will be reduced, but the former will be reduced more drastically than the first one. Thus, to fulfill the energy condition it is necessary to increase the applied strain level. This criterion has also been successfully used to predict the evolution of crack density with the strain level (Hashin, 1996; Nairn, 2000).

The main weak point of this criterion is the a priori selection of the crack length after the onset. Although this selection for the present problem seems straightforward, this is not usual for other problems. In fact, one of the first applications (Aveston et al., 1971) of this criterion used a very arbitrary crack length. Additionally, the jump in crack length needs to be verified experimentally.

2.4. Model based on a combination of a stress criterion and an incremental energy criterion

This model is based on combining two of the criteria described previously: a stress criterion and an incremental energy criterion. At present, this criterion is typically denoted as coupled criterion and is used for many other problems. According to this criterion (Leguillon, 2002) the two criteria are necessary conditions for the crack onset and their simultaneous fulfillment represents a sufficient condition for a crack onset. Similarly to the incremental energy criterion discussed previously, the coupled criterion assumes a finite jump in the crack length. However, in contrast to the incremental energy criterion, the value for this critical length is not a material or geometric property but a result of the analysis. The stress criteria prescribe a minimum value for stresses at those points where the crack onset is going to occur. Both the stress and the energy criteria depend on the crack length after the onset, thus the critical crack length can be obtained by minimizing the critical load fulfilling the two criteria simultaneously. This criterion was briefly evoked for the problem studied here in the context of a work dedicated to other problem by Leguillon (2002) and further developed for the problem of transverse cracking by García et al. (2014). The critical strain can be expressed as the combination of the two

previous criteria: stress criterion (2) and a generalization of the incremental energy criterion (9),

$$\varepsilon_{yy}^{\mathrm{c}} = \max\left[\frac{Y_{\mathrm{t}}}{E_{22}}\frac{1-\nu_{12}\nu_{21}}{1-\nu_{12}\nu_{21}\frac{1+\frac{t_0}{t_{90}}}{1+\frac{E_{22}}{E_{11}}\frac{t_0}{t_{90}}}}, \sqrt{\frac{G_{\mathrm{c}}}{E_{22}t_{90}}\min_{0\leq a/t_{90}\leq 1}\left(\frac{a/t_{90}}{\int_0^{a/t_{90}}\hat{G}(a'/t_{90})\mathrm{d}(a'/t_{90})}\right)}\right]. \tag{10}$$

Although the original model, from which the expression (10) derives, is based on a 2D generalized plane strain model, the accuracy of this model in comparison with a 3D model was confirmed by García et al. (2016). According to this result, even in the case with the crack onset appearing at the free edge, the expression (10) gives a very accurate approximation for the critical strain.

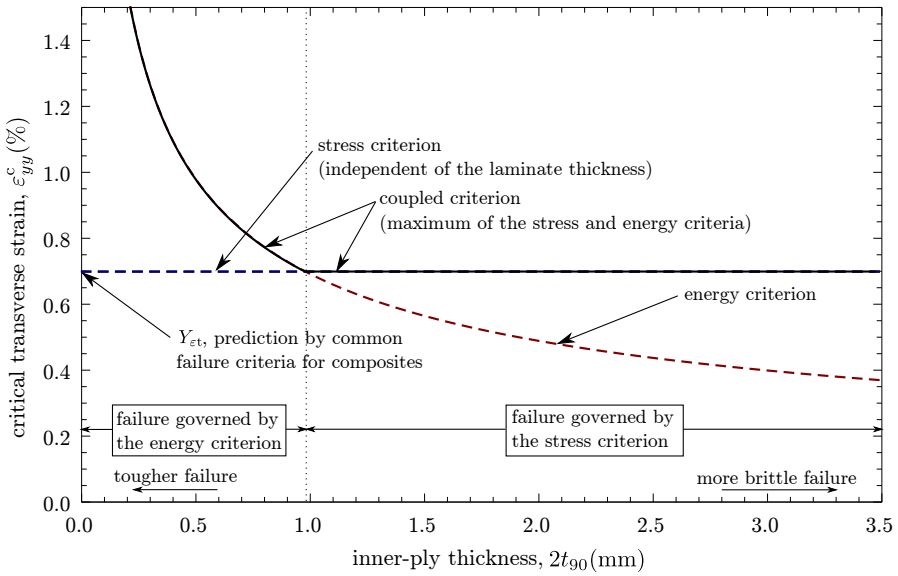

Figure 4: Model based on an combination of a stress criterion and an incremental energy criterion, Leguillon (2002); García et al. (2014). Prediction of the critical transverse strain as a function of the inner-ply thickness for cross-ply laminates $[0_n/90_{n/2}]_{\mathrm{s}}$ of AS4/8552 carbon/epoxy with properties in Table 1.

This model is able to predict a size effect inherited from the incremental energy criterion. The size effect predicted by this model can be observed in Figure 4, where the critical strain $\varepsilon_{yy}^{\mathrm{c}}$ is plotted as a function of the inner-ply thickness $2t_{90}$. The dependence with the inner-ply thickness is very similar to that predicted by the incremental energy criterion and the inherent flaw mechanics. The main advantage of the coupled criterion over the other two is that this criterion is not restrained to particular problems and it has been applied successfully to many divers problems and materials, see García (2014); Weißgraeber et al. (2016) for reviews.

2.5. Combination of a stress criterion and an stochastic analysis

It is well known that the properties used in a macroscopic mechanic analysis as Elastic Modulus, Tensile Strength, Fracture Toughness and others are actually average values. Thus, the main properties used in the previous models are subjected to a spatial variation given by statistical distributions. This fact is also a source for size effect. The reason is that if the size increases, the probability of finding extreme values for the defect sizes or the properties involved in the failure as strength or fracture toughness increases. Thus, the statistical variation of the properties is associated to a higher strength of smaller specimens as observed in the experiments in cross-ply laminates.

The most common model based on this idea is the application of a stress-based criteria, see Section 2.1, assuming a volumetric Weibull distribution for the transverse strength Y_{t}, see Manders et al. (1983). Assuming that the stresses are uniform through the width and thickness, the cumulative distribution function of failure

S for a given volume and stress level is:

$$S = 1 - \exp\left[-\left(\frac{\sigma_{yy}^{(90)}}{\sigma_0/\left(t_{90}WL\right)^{1/w}}\right)^w\right] \tag{11}$$

where $\sigma_{yy}^{(90)}$ is the tension in the transverse ply. The parameters $\sigma_0/\left(t_{90}WL\right)^{1/w}$ and w correspond to the scale and shape parameters of the Weibull distribution. These parameters can be extracted using different methods as linear regression, weighted least square, moments method and maximum likelihood method. All these methods are based on a wide batch of tests in order to measure with certainty the average value and the variability. The moment method is the most suitable if normalized tests for strength are available. The reason is that the moment method estimates the Weibull parameters from the average value and standard deviation of the strength, which are commonly provided with test results.

According to the moment method, see e.g. Tiryakioğlu (2008), the value of w can be estimated by solving the next equation:

$$\frac{Y_{\mathrm{t}}}{s_{Y_{\mathrm{t}}}} = \frac{\Gamma\left(1+\frac{1}{w}\right)}{\sqrt{\Gamma\left(1+\frac{2}{w}\right) - \left(\Gamma\left(1+\frac{1}{w}\right)\right)^2}} \tag{12}$$

where Y_{t} and $s_{Y_{\mathrm{t}}}$ are the average transverse strength and the standard deviation, and Γ denotes the Gamma function. Once the shape parameter w is estimated, the scale parameter σ_0 can be calculated using:

$$\sigma_0 = \left(t_{90}^* W^* L^*\right)^{1/w} \frac{Y_{\mathrm{t}}}{\Gamma\left(1+\frac{1}{w}\right)} \tag{13}$$

where t_{90}^*, W^* and L^* correspond to the geometric parameters of the unidirectional specimens used to obtain Y_{t}.

Thus, an expression for the critical strain $\varepsilon_{yy}^{\mathrm{c}}$ analogous to that presented for previous models can be obtained by introducing the approximation for $\sigma_{yy}^{(90)}$ used in Section 2.1,

$$\varepsilon_{yy}^{\mathrm{c}} = \frac{Y_{\mathrm{t}}}{E_{22}} \frac{1-\nu_{12}\nu_{21}}{1-\nu_{12}\nu_{21}\frac{1+\frac{t_0}{t_{90}}}{1+\frac{E_{22}}{E_{11}}\frac{t_0}{t_{90}}}} \left(-\frac{\log(1-S)}{\Gamma\left(1+\frac{1}{w}\right)} \frac{t_{90}^*}{t_{90}} \frac{W^*}{W} \frac{L^*}{L}\right)^{1/w} \tag{14}$$

where the expression for σ_0 in (13) has been introduced to make appear Y_{t}, the ratios of geometric ratios $\frac{t_{90}^*}{t_{90}}$, $\frac{W^*}{W}$ and $\frac{L^*}{L}$. Note that, in contrast to the previous method, the value of $\varepsilon_{yy}^{\mathrm{c}}$ in this model depends on the value chosen for the probability of transverse crack onset S. The value for S represents the probability that the first transverse crack onset occurs at given strain level $\varepsilon_{yy}^{\mathrm{c}}$ or below.

This method have been proposed by several authors also to predict the evolution of crack density with the strain level, Manders et al. (1983); Takeda and Ogihara (1994); Li and Wisnom (1997). The main differences between these authors are the procedures for the estimation of the Weibull parameters.

The size effect predicted by this model is showed in Figure 5. For a fixed probability of failure S, the critical strain $\varepsilon_{yy}^{\mathrm{c}}$ is proportional to $1/{t_{90}}^{1/w}$. By contrast, in some of the models discussed previously, Section 2.2, 2.3 and 2.4, the value of $\varepsilon_{yy}^{\mathrm{c}}$ is proportional to $1/{t_{90}}^{1/2}$. Thus, the shape parameter w modulates in this model the size effect.

The main advantage of this model with respect to the previous ones is that the value of $\varepsilon_{yy}^{\mathrm{c}}$ is associated to a value of the probability. This fact allows taking into account the natural scattering observed in experiments and using it in the analysis. However, this model requires a large number of tests to characterize adequately the parameters involved in the prediction. The moment method used here is the least demanding method in terms of parameters required. However, the majority of works using this model in the literature have required extensive batch tests and subsequent fitting. In addition, all these methods to extract the variability in the transverse strength assume that the variability in the experimental results is exclusively associated to the transverse strength scattering. However, other sources can contribute to the variability as sensor inaccuracies or specimen geometric tolerances. If these effects are relevant, the variability can be overestimated.

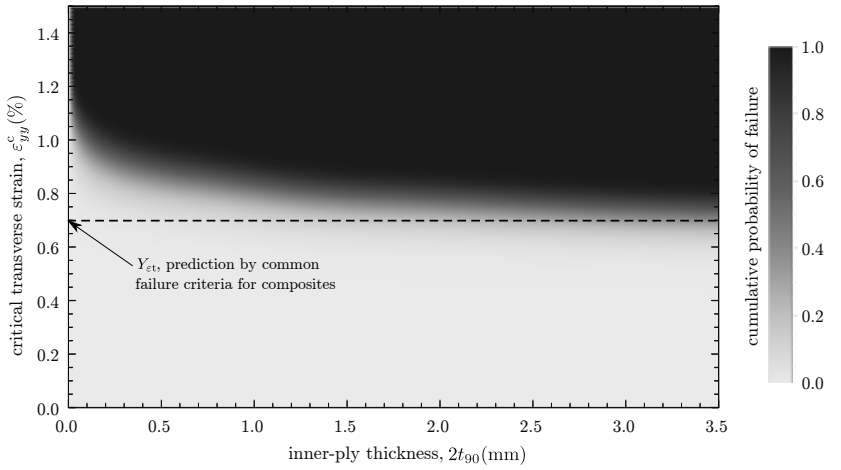

(a) Cumulative probability of failure

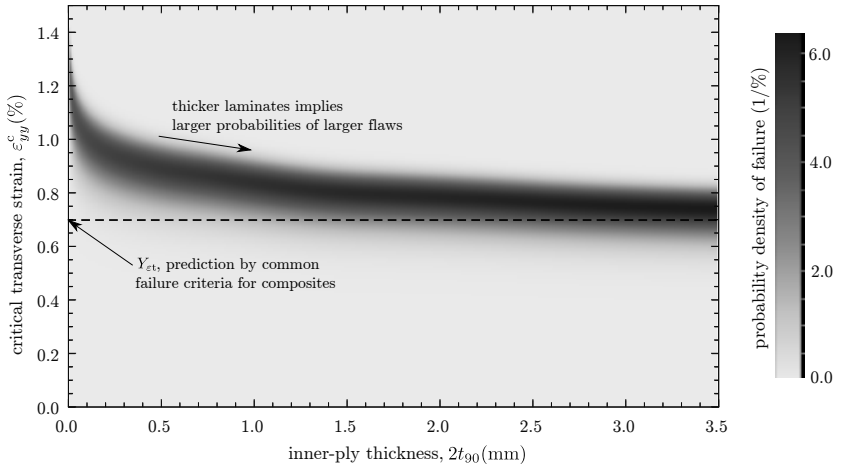

(b) Probability density of failure

Figure 5: Model based on a stochastic analysis of the failure, Weibull (1939); Li and Wisnom (1997). Prediction of the critical transverse strain as a function of the inner-ply thickness for cross-ply laminates $[0_n/90_{n/2}]_s$ of AS4/8552 carbon/epoxy with properties in Table 1.

2.6. Considering residual thermal stresses in previous theoretical models

Residual thermal stresses in current composites can be very relevant due to the use of thermoset resins cured at a relatively high temperature and the anisotropy of the thermomechanical properties. Some of the previous theoretical models originally considered the inclusion of these residual stresses. However others did not include the residual thermal stresses because they were not relevant in the seminal experiments by Parvizi et al. (1978) due to the material and fabrication procedure employed. In the context of the present work, a common correction to take into account the residual thermal stresses in cross-ply laminates will be implemented for the sake of comparison.

According to García et al. (2018), the inclusion of residual thermal stresses in theoretical models based on stress criterion, energy criterion or their combination is equivalent to add a residual equivalent strain $\varepsilon^{\Delta T}$ to the mechanically imposed one ε_{yy}. This residual equivalent strain can be calculated using the Laminate Theory as,

$$\varepsilon^{\Delta T} = \alpha_2 \Delta T \left(\frac{1-\nu_{12}\nu_{21}}{1-\nu_{12}\nu_{21}\frac{1+\frac{t_0}{t_{90}}}{1+\frac{E_{22}}{E_{11}}\frac{t_0}{t_{90}}}} k^{(90),\Delta T} - k^{0,\Delta T} \right). \tag{15}$$

where α_2 is the transverse coefficient of thermal expansion (CTE) and ΔT is the temperature change. The function $k^{0,\Delta T}$ is

$$k^{0,\Delta T}\left(\frac{E_{22}}{E_{11}},\nu_{12},\frac{t_0}{t_{90}},\frac{\alpha_1}{\alpha_2}\right)=\frac{k_1\left(\frac{E_{22}}{E_{11}},\nu_{12},\frac{t_0}{t_{90}},\frac{\alpha_1}{\alpha_2}\right)-k_2\left(\frac{E_{22}}{E_{11}},\nu_{12},\frac{t_0}{t_{90}},\frac{\alpha_1}{\alpha_2}\right)}{k_3\left(\frac{E_{22}}{E_{11}},\nu_{12},\frac{t_0}{t_{90}},\frac{\alpha_1}{\alpha_2}\right)}, \tag{16}$$

where α_1 is the longitudinal CTE. The functions k_1, k_2 and k_3 are given by the expressions

$$k_1=\frac{t_0}{t_{90}}\frac{\alpha_1}{\alpha_2}+\frac{E_{22}}{E_{11}}\left(1+\left(\frac{t_0}{t_{90}}\right)^2\frac{\alpha_1}{\alpha_2}+\nu_{12}\frac{t_0}{t_{90}}\left(1-\frac{\alpha_1}{\alpha_2}\right)\right), \tag{17a}$$

$$k_2=\left(\frac{E_{22}}{E_{11}}\right)^2\left(\frac{t_0}{t_{90}}\left(\nu_{12}\left(1-\frac{\alpha_1}{\alpha_2}\right)-1\right)+\nu_{12}^2\left(1+\frac{t_0}{t_{90}}\right)\left(1+\frac{t_0}{t_{90}}\frac{\alpha_1}{\alpha_2}\right)\right), \tag{17b}$$

$$k_3=\frac{t_0}{t_{90}}+\frac{E_{22}}{E_{11}}\left(1+\left(\frac{t_0}{t_{90}}\right)^2\right)-\left(\frac{E_{22}}{E_{11}}\right)^2\left(\nu_{12}^2\left(1+\frac{t_0}{t_{90}}\right)^2-\frac{t_0}{t_{90}}\right). \tag{17c}$$

and $k^{(90),\Delta T}$ by

$$k^{(90),\Delta T}\left(\frac{E_{22}}{E_{11}},\nu_{12},\frac{t_0}{t_{90}},\frac{\alpha_1}{\alpha_2}\right)=\frac{1-\frac{E_{22}}{E_{11}}\left(\frac{t_0}{t_{90}}\left(\nu_{12}\left(1-\frac{\alpha_1}{\alpha_2}\right)-1\right)+\nu_{12}^2\left(1+\frac{t_0}{t_{90}}\frac{\alpha_1}{\alpha_2}\right)\right)}{\left(1-\frac{E_{22}}{E_{11}}\nu_{12}^2\right)\left(\frac{E_{22}}{E_{11}}\frac{t_0}{t_{90}}+1\right)}. \tag{18}$$

Thus, the previous theoretical models can be extended to take into account residual thermal stresses by simply adding the value of $\varepsilon^{\Delta T}$ to the right-hand side of the corresponding expressions in (2), (7), (9), (10) and (14).

3. Specimen description

A set of specimens was designed, fabricated and tested with the objective of evaluating the size effect in cross-ply laminates. The design of specimens was based on the idea of spanning a spectrum of thicknesses as wide as possible. The typical tensile specimen with tabs has been used, taking ASTM Standard D3039 (2006) as reference, see Figure 1. It is composed by a rectangle of the laminate with lengths $L \times W$. $\pm 45^\circ$ glass/epoxy tabs were bonded to the extremes of the specimen where the tensile testing machine grips it, in order to avoid a premature failure at these zones. These tabs are rectangular with size $L_g \times W$ and thickness t_g. The tabs length are defined with the aim of assuring the correct transmission of the load from the tabs to the laminate without failure of the adhesive. Within a range, a larger adhesion surface is able to transmit higher loads. According to the experimental results found in the literature, the critical strain is of a similar order for all the laminates. Thus, since the thickest laminates require higher loads to be applied for the same strain level, the tabs were sized to be long enough for these laminates. The lay-up configuration was selected in accordance with the following conditions:

- All the specimens tested should be geometrically similar in order to study the size effect avoiding the effect of other parameters. Parvizi et al. (1978), such as the majority of other authors, kept fixed the outer-ply thickness t_0 varying the inner-ply thickness t_{90} to study the size effect. However, a dimensional analysis of the problem shows that all the length ratios has to be kept fixed in order to adequately study the size effect. An exception can be assumed regarding the length L and width W of the specimen when they are large and wide enough compared with t_{90}. This is not the case of t_0, which is typically of the order of t_{90} in experiments in the literature. As a consequence, rigorously, the ratio t_0/t_{90} should be kept fixed when the size effect is studied. If it is not, a mixed influence of the size (thickness) and the variation of t_0/t_{90} is actually obtained.

- In order to span a range of thicknesses as wide as possible, the thinnest laminate should have a single layer of prepreg as inner ply. On the other extreme, sufficiently thick laminates should be also tested.

Given that at least a layer at each side has to be placed for the thinnest laminate and that a single layer composes the inner ply, the most adequate laminate in terms of material use is $[0/90/0]$. Note that this corresponds to $t_0/t_{90} = 2$. Since this ratio has to be fixed, the lay up configurations are given by $[0_n/90_n/0_n]$. According to the experimental observations reported in the literature, the size effect is more relevant for the thinnest laminates, see e.g. Parvizi et al. (1978). Due to this, test specimens were fabricated for $n = 1, 2, 3, 4, 5$. On the other extreme, experiments show a very low size effect for the thickest specimens. In addition, these laminate requires much more material. Thus, in order to save material while the experiments span a wide enough range of thicknesses, three lay up configuration were fabricated for $n = 7, 10, 16$. Based on the experimental results in the literature, it is assumed that the laminates with $n = 16$ are thick enough to capture the tendency for thick laminates.

A laminate was manufactured for each value of n in Table 1. The laminates were made by stacking up unidirectional layers of carbon fiber tape (Hexcel AS-4) preimpregnated in epoxy resin (Hexcel®8852) with a resin volumetric content of $31-35\%$, a nominal cured thickness per ply of $0.17-0.19$ mm and an areal weight of $268-308$ g/m^2. If the laminate contained more than 5 layers, every 5 layers the partial laminate was subjected to vacuum to avoid the presence of air bubbles. After the full stacking of the laminates, they were introduced in a vacuum bag on an aluminum plate and a set of tests were carried out to detect any vacuum leak. All the laminates were cured simultaneously in an autoclave using the manufacturer's recommended cure cycle. The tabs, which are made from glass fiber fabric impregnated with epoxy, were cured independently. Once both laminates and tabs were cured and the edges of the laminates were cut and dismissed, the tabs were bonded to the laminates using an adhesive layer. The whole set was introduced in a hot-plate press to cure the adhesive. At least 7 specimens were cut from each laminate with the aid of a diamond disc saw.

4. Testing procedure and data extraction

Once the specimens were manufactured, one of their edges was entirely sanded and polished to allow post testing observations of the transverse cracks. The tests were run using an electromechanical testing machine Instron 4483. A monotonic tensile load was applied under displacement control at a cross-head rate of 0.5 mm/min. During the test, a load cell Instron 2525-112 with a maximum capacity of 150 kN was used to record the load applied to the specimen. The cross-head displacement was also measured and its value recorded. To obtain a more accurate measure of the strain, two strain gauge extensometers, Instron 2630-112 with 50 mm gauge length and Instron 2630-107 with 25 mm gauge length were also used to measure the strain through the relative displacement between two points.

The onset of cracks in the inner ply of the cross-ply laminates tested does not entail a significant reduction in the global stiffness of the specimen. This is due to the very low contribution of the inner ply to the stiffness of the specimen as a consequence of the high contrast between the longitudinal and transverse Young's moduli and that the thickness of the plies are similar. As a consequence, the onset of a crack in the inner ply cannot be detected by inspecting the load-strain curve. Several alternative methods have been used in the experiments reported in the literature as X-ray in the case of opaque laminates or direct observation for transparent laminates. Another alternative is the use of acoustic emission to detect damage events, which is very common in composites, see e.g. Wevers and Surgeon (2000) for a review. This was the main method implemented in this work. The acoustic emission was measured here by attaching a contact microphone to the specimen. The voltage at the contact microphone V^{mic} was recorded at 44100 Hz enabling a very accurate detection of any event producing an acoustic wave in the specimen.

The post-mortem observation at the optical microscope showed some differences in the cracking process between the specimens corresponding to different values of n, i.e. with different inner-ply thicknesses. In the following, the details found for each n are described,

- For the thinnest laminates ($n = 1$) a single strong sound peak was found, which was followed by the global failure of the specimen. In the majority of the specimens, a large delamination at both interfaces connected by a single transverse crack is found, see e.g. Figure 6a. Since both phenomena occurs almost simultaneously, it is difficult to observe which of them occurs previously. Thus, it is not known which of these damage events originates the other, and consequently it is not clear if the failure mode is controlled by transverse cracking. Within this high level of uncertainty, some evidences shown in Figure 6a lead to believe that the first failure for $n = 1$ is the delamination. The main evidence is the angle formed

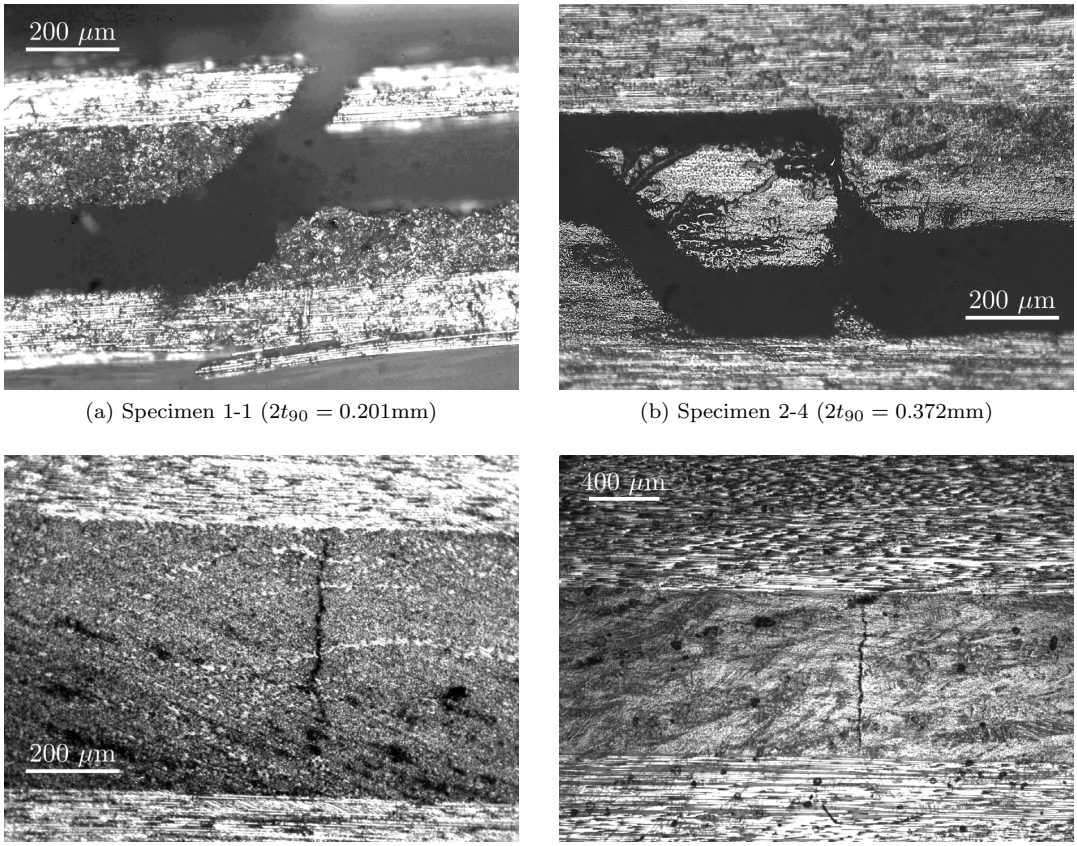

(a) Specimen 1-1 ($2t_{90} = 0.201$mm)

(b) Specimen 2-4 ($2t_{90} = 0.372$mm)

(c) Specimen 3-1 ($2t_{90} = 0.570$mm)

(d) Specimen 5-2 ($2t_{90} = 0.985$mm)

Figure 6: Examples of post-mortem micrographs obtained after the acoustic detection of transverse crack onset.

between the transverse crack and the interface. If the interface was not damaged previously, then, due to the symmetry, it would be reasonable to think that the first transverse crack initiates approximately perpendicular to the load direction. In fact, this is the case for larger values of n, see e.g. Figures 6c and 6d. However, the case for $n = 1$ in Figure 6a shows a transverse crack which is far from being perpendicular to the load. The fact of that the first observed transverse crack is oblique could be explained by the bending moment produced when a sudden delamination occurs at one of the interfaces. This delamination would kink out the interface towards the inner ply with an angle which would be affected by the bending moment linked to the lack of symmetry caused by the delamination. Other evidence supporting this hypothesis is the continuity of the angle of this crack transversing also the outer ply. This is coherent with the sequential process of failure described: a delamination which is followed by a transverse crack. The similitude of the crack angles at the inner and outer plies implies that the bending moment causing this angle was similar before and after the crack going through the interface. As discussed previously, the bending moment is given mainly by the presence of the delamination at the interface. Thus, if the bending moment is similar, it implies that the delamination does not change significantly during the process of inner and outer ply cracking. The process would be: delamination, kink out the interface toward the inner ply and cracking of the outer ply. Thus, the initiation of this failure mechanism is not governed by the transverse cracking, but it is by the delamination probably associated to the free-edge effect, see e.g. Martin et al. (2010).

- The behavior found for $n = 2$ can be considered as a transition between the behavior observed for $n = 1$ and for thicker laminates. Whereas some specimens showed the same behavior that for $n = 1$, others showed the usual transverse cracking observed for larger values of n. Moreover, in some cases, see e.g. Figure 6b, the two behaviors seem to appear in the same specimen. Note that at this micrograph two transverse cracks are visible. Whereas the transverse crack on the left has a similar angle that the transverse crack described for $n = 1$, the transverse crack on the right is perpendicular to the load in the majority of its

length. In addition, two delaminations appear, being connected by both transverse cracks. This complex behavior can be explained by the next sequence,

1. A transverse crack onset occurs which corresponds to the crack on the right shown in Figure 6b.
2. The onset of a delamination occurs probably associated to the free-edge effect.
3. The delamination kinks out the interface toward the inner ply, which corresponds to the transverse crack on the left.
4. A new delamination occurs at the other interface due to the proximity of the new transverse crack.
5. The new delamination reaches the first transverse crack connecting both transverse cracks.

- For larger values of $n = 3, 4, 5, 7, 10, 16$, the post-mortem observation at optical microscope shows clearly a set of transverse cracks perpendicular to the load, see Figures 6c and 6d. Actually the perpendicularity between the crack and the load direction observed here in a post-mortem micrograph does not imply necessarily that crack and load were perpendicular when the specimen was loaded as observed by Tessema et al. (2018). However, in contrast with the specimens tested by Tessema et al. (2018) where the 90° ply is surrounded by two plies with different orientations (breaking the "local symmetry" around the 90° ply), in the test studied here it is more plausible the transverse crack onset occurs perpendicular to the loading direction in absence of delamination. These transverse cracks are sometimes accompanied by small delaminations at the interface near the crack tip very probably originated by the stress concentration at the interface when a transverse crack approaches it, see París et al. (010a,b) for a detailed explanation of this phenomenon. Excluding the critical values of strain studied in next section, the only relevant difference between the behavior observed for the specimens corresponding to these values of n is the frequency of the crack onsets. It is observed that the frequency decreases for thicker laminates. The cause is that for these laminates, the specimens are shorter in dimensionless terms since the length has not been scaled with the thickness. As a consequence, the presence of a transverse crack affects a large part of the length for large n making more difficult the subsequent transverse crack onsets.

In few cases the critical strain for which the process of transverse cracking begins can be easily recognized because the acoustic peaks appears clearly above a certain level of strain. However, in general the critical strain is not as clear. In most cases, a large peak, corresponding to a strain damage event, was not immediately followed by contiguous peaks. Therefore, it is not clear whether the value of "first transverse crack onset" should be associated to the very first isolated peak or to the appearance of contiguous peaks. Thus, it is necessary to establish a criterion for what is going to be considered as the first crack and as a consequence which strain is considered as critical. In this work two different critical value for the strain are taken as reference:

- The critical strain ε_{yy}^{c1} leading to the very first transverse crack onset. This corresponds to the first peak associated to a transverse crack onset without taking into account that the damage event is isolated. This crack onset could correspond to a crack initiated from an unusually large flaw. This type of crack onset would be out of the scope of the onsets being claimed to be predicted by the FFM model discussed here.

- The critical strain ε_{yy}^{c2} leading to a transverse crack onset which is almost immediately followed by other crack onsets. Due to the length of the laminate in comparison with the other lengths, it is expected that if the conditions to expect a crack onset are fulfilled, several crack onsets adequately separated along the length are also expected. The crack onsets are not necessarily (strictly speaking) simultaneous in view of a slight variability of the material properties along the specimen length. In this case, it is necessary to define what is considered as approximately simultaneous. On the one hand, it is necessary to define a sufficiently wide range to capture two crack onsets whose difference is based on the material property variability. On the other hand the range has to be narrow enough to reject crack onsets due to unusually large flaws. Thus, based on the observation of the results obtained here, the next conditions are followed to define a crack onset as the first one:

  - A second crack onset followed the first one within the subsequent 5 seconds (corresponding approximately to a strain increment of 0.0026%).
  - A third one within the subsequent 10 seconds (corresponding approximately to a strain increment of 0.0052%).

– A fourth one within the subsequent 30 seconds (corresponding approximately to a strain increment of 0.0156%).

In what follows the results will show both critical strains, because whereas ε_{yy}^{c1} is *a priori* highly affected by the randomness in the presence of large flaws. This is actually the value for the critical strain which is the most independent of additional assumptions. In addition, it is interesting to observe the difference between both strains in order to evaluate the importance of the flaws in the cracking process.

5. Results and Discussion

The experimental results recorded for the two critical values of the strain are presented and discussed here. The experimental results are compared with the critical strain predicted by the theoretical models described in Section 2.

Figure 7 shows the experimental results obtained for the two critical strains ε_{yy}^{c1} (first crack onset) and ε_{yy}^{c2} (first simultaneous crack onsets) defined previously as a function of the inner-ply thickness ($2t_{90}$) in comparison with the main theoretical models. The measured values obtained for the two critical strains ε_{yy}^{c1} and ε_{yy}^{c2} are detailed in Table A.2 in Appendix A. In addition, the inner-ply thickness of each specimen is defined as the mean of the measured thicknesses at three distant points with the aid of the optical microscope.

Values for ε_{yy}^{c1} and ε_{yy}^{c2} were obtained for the majority of the specimens. However, some problems arose with measurements of ε_{yy}^{c2} for certain values of n and that is why these values are missing for some specimens, as can be observed in Figure 7 and Table A.2. In the case of the specimens corresponding to $n = 1$, values for ε_{yy}^{c2} are missing for all of them. This is due to the failure sequence described for $n = 1$. These specimens only show a single sound peak corresponding to a transverse crack before the global failure. Moreover this transverse crack is probably associated to a previous delamination as discussed previously. The fact that only one transverse crack onset is detected makes it impossible to fulfill the conditions defined for ε_{yy}^{c2}. This critical strain could not be obtained for some specimens corresponding to $n = 10$ and $n = 16$. In these cases, these values are missing due to the premature failure of the adhesive which bonds the tabs and the laminate due to the high loads necessary to provide a similar level of strain for thick specimens. Note that unlike the case $n = 1$, the lack of a value for ε_{yy}^{c2} for thick specimens is not due to a different behavior of the failure process but because of a phenomenon associated to the testing procedure.

Property	Value	Reference
E_{11} (GPa)	127.277	Marlett (2010)
E_{22} (GPa)	9.239	Marlett (2010)
ν_{12}	0.302	Marlett (2010)
ν_{23}	0.4	similar material in Soden et al. (1998)
G_{12} (GPa)	4.826	Marlett (2010)
Y_{t} (MPa)	63.9	Marlett (2010)
$s_{Y_{\mathrm{t}}}$ (MPa)	6.05	Marlett (2010)
W^* (mm)	25.0	Marlett (2010)
L^* (mm)	125.0	Marlett (2010)
t_{90}^* (mm)	1.016	Marlett (2010)
G_{c} (N/m)	248	value for initiation in Renart et al. (2011)
α_1 (°Cμm/m)	-1	similar material in Soden et al. (1998)
α_2 (°Cμm/m)	26	similar material in Soden et al. (1998)
ΔT (°C)	-157	autoclave

Table 1: Material properties for AS4/8852 carbon/epoxy.

In general, a decreasing tendency of both critical strains when the laminates are getting thicker can be observed in the results in Table A.2. This tendency is clearer for the thinnest specimens in spite of a larger dispersion was found for these laminates. For the thick specimens the critical strain seems to tend to a fixed value around $0.1 - 0.3\%$. Note that this value is significantly lower than the unidirectional critical transverse strain $Y_{\varepsilon \mathrm{t}} = Y_{\mathrm{t}}/E_{22} = 0.69\%$ of the lamina, see Table 1. This is caused by the presence of high residual stresses

in the inner ply due to the cooling-down from the curing to the room temperature, as will be seen in the following.

The predictions by the main theoretical models described in Section 2 are plotted in Figure 7 for comparison with the experimental results. The dashed curves from Figure 7a to Figure 7d and the probability of failure represented in Figure 7e correspond to the theoretical models without considering residual thermal stresses.

To implement the expressions for the critical strain $\varepsilon^{\mathrm{c}}_{yy}$ given for each model in Section 2, the material properties are taken from different sources: The longitudinal E_{11} and transverse E_{22} Young's moduli and the major Poisson's ratio ν_{12} for this material obtained by Marlett (2010) following the ASTM Standard D3039 (2006) are taken here as a reference. The in-plane shear modulus G_{12} is also taken from the report by Marlett (2010) who measured it using the ASTM Standard D3518 (2007). Unfortunately, no value for the through thickness Poisson's ratio ν_{23} was found in the literature. The value given by Soden et al. (1998) for a similar material is taken as a reference. Although this value is necessary for the FFM model, the results are not expected to vary significantly in the worst scenario of a large error in this estimation of ν_{23}. Similarly, the values for the longitudinal α_1 and transverse α_2 coefficients of thermal expansion are identified with the values given by Soden et al. (1998) for a similar material. With regards to the unidirectional tensile transverse strength Y_{t}, the value measured by Marlett (2010) was taken as a reference. In addition the standard deviation $s_{Y_{\mathrm{t}}}$ of the tensile transverse strength was extracted from Marlett (2010) along with the the thickness t^*_{90}, width W^* and length L^* of the specimens used to measure Y_{t}. The transverse fracture toughness G_{c} for this material was measured by Renart et al. (2011) with Double Cantilever Beam tests according to the ISO Standard 15024 (2001). The value taken here corresponds to the value obtained for the initiation denoted as 5%MAX. Actually, Renart et al. (2011) gives two values for 5%MAX, either using end blocks bonded to the specimen as indicated in the ISO Standard 15024 (2001) or a novel set of hinges clamped to the end of the specimens. Since the end blocks are currently indicated by the standards, the value given using them is taken here. Table 1 presents the values for the material properties assumed here for AS-4/8852 and summarizes the references from which these values are extracted.

For the implementation of some of the theoretical models it is also necessary to compute some energetic results. In Section 2 all of them were related with a dimensionless energy release rate $\hat{G}$. The computation of $\hat{G}$ was obtained using an interpolation based on the results of a very accurate Boundary Element Method (BEM) model (Blázquez et al., 2008), see results in Appendix B.

The comparison between the experiments and the predictions given by the theoretical models without considering residual thermal stresses shows that the tendency is well predicted by all models with the exception of that based on a pure stress criterion. However, all models strongly overestimate the critical strain for which the first crack onsets occur. The reason for this overestimation is probably the effect of the residual thermal stresses.

The effect of the residual thermal stresses can be introduced in all models in the form proposed in Section 2.6. The value $\varepsilon^{\Delta T}$ necessary to introduce the influence of the residual stresses is calculated by using the expression (15) as a function of the thermoelastic material properties, t_0/t_{90} and the difference between the curing temperature and the room temperature ΔT. The following value is obtained by using the data from Figure 1 and Table 1.

$$\varepsilon^{\Delta T} = 0.422901\%. \tag{19}$$

Note that this value represents 61.1% of the unidirectional critical transverse strain $Y_{\varepsilon \mathrm{t}} = Y_{\mathrm{t}}/E_{22}$, i.e. a non-negligible part of the nominal strength of the inner ply is reduced due to the curing process.

The solid curves in Figures 7a to 7d and the probability of failure represented in Figure 7f correspond to the theoretical models considering residual thermal stresses, which greatly improves the agreement between models and experiments. In general the agreement between models and experiments has improved greatly. Now, the majority of models slightly overestimate the critical strain for which the very first crack onset occurs. However, the majority of them approximate well or even underestimate the critical strain for which the first simultaneous cracks onsets appear. In our opinion, the very first crack onset is originated by the presence of an unusual large flaw and the majorty of models studied here do not take into account the presence of these flaws. In what follows the comparison is discussed individually for each model.

The comparison between the model based on pure stress criterion, shown in Figure 7a, and experiments shows a good agreement for the thickest laminates. However, the stress criterion is not able to predict the strong size effect found for the thinnest laminates. Whereas this error could be acceptable in some applications

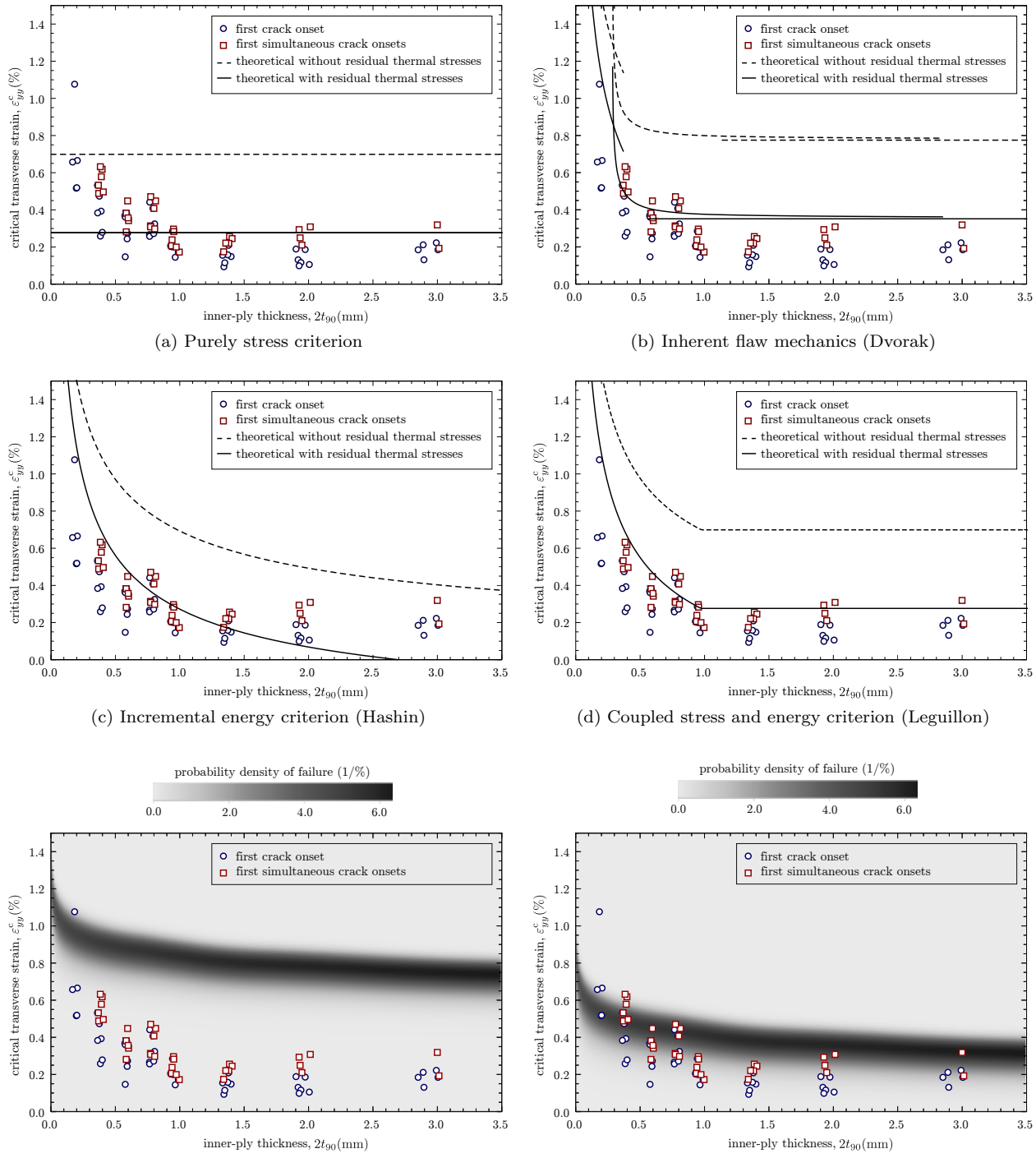

(a) Purely stress criterion

(b) Inherent flaw mechanics (Dvorak)

(c) Incremental energy criterion (Hashin)

(d) Coupled stress and energy criterion (Leguillon)

(e) Stochastic criterion (Weibull) without including residual thermal stresses

(f) Stochastic criterion (Weibull) with including residual thermal stresses

Figure 7: Comparison of the experimental results obtained here with the predictions given by the main theoretical models.

because it is on the safe side, this criterion is obsolete to study a new generation of laminates composed by ultra-thin plies assuming that the present results are extrapolable to these plies.

Figure 7b shows the comparison between the inherent flaw mechanics (Dvorak) model and the experiments. This model is able to predict the size effect, particularly accurately for the thinnest laminates. Nevertheless, the prediction overestimates the in-situ strength for mid-thickness and thick laminates. This fact is a consequence of the 1.12 factor between the unidirectional transverse strength and the in-situ strength predicted for cross-ply laminates.

The incremental energy criterion (Hashin) is compared with experiments in Figure 7c. This model is also able to predict the critical transverse strain for the thinnest laminates with a slight overestimation. However, its predictions for the thickest laminates are clearly underestimated. In fact, for the thickest laminates this criterion predicts that crack onset will occur after the fabrication before applying any mechanical load.

The prediction of the coupled stress and energy criterion (Leguillon) is plotted in Figure 7d along with the experiments. The coupled criterion shows a good agreement, in general, with a slight overestimation in the most part of all the range of thicknesses studied. The clear change of tendency predicted by the coupled criterion is also observed in the experiments around the same values of thickness.

The density of the probability of failure given by the stochastic criterion based on the Weibull distribution is represented in Figure 7f against the experimental results. The general tendency is well captured by this model. The prediction for the thickest laminates presents a good agreement with experiments. However, the size effect predicted for the thinnest laminates underestimates the size effect found in the experiments. It is necessary to remark that the application of this criterion here was based on extracting the Weibull parameters from the mean and standard deviation of the unidirectional transverse strength. However, this criterion was typically presented in the literature as based on the analysis of the variability of experimental results for cross-ply laminates themselves. Since this last procedure requires a large amount of tests and fitting in comparison with the other models shown here, it is considered here more practical to compare it with a similar number of data.

6. Concluding remarks

The new experimental results in cross-ply laminates of AS4/8552 carbon/epoxy confirm a clear size effect on transverse cracking under tension. In particular, the observed strength of the transverse ply increases strongly for the thinnest plies. This observation justifies the development of the new ultra-thin plies which would inhibit the transverse cracking in these laminates. Since transverse cracking is typically one of the first steps of some failure mechanisms, the inhibition of this step would increase the global strength of the laminate.

The comparison of the experimental results with the theoretical models shows that the purely stress-based criteria, which are the most used in practical applications, predicts the strength on the safety side but underestimates the strength for the thinnest laminates. This implies that the stress criteria are useful for the current laminates but it will not allow to take advantage of the laminates made of ultra-thin plies. In contrast, the other criteria do predict the strong size effect with more or less accuracy depending on the studied range. The inherent flaw mechanics (Dvorak) model agrees well the experimental results for the thinnest laminates but overestimates of the strength for the thicker ones. The incremental energy criterion (Hashin) also predicts well the strength for the thinnest laminates but, in this case, underestimates the strength for the thickest laminates. The coupled criterion of the finite fracture mechanics (Leguillon) predicts well but with a small overestimation the strength in most part of the range of thickness studied. Finally, the stochastic model gives a good approximation of the experimental results but underestimates the size effect.

All the theoretical models have been calculated including residual thermal stresses and without them. The inclusion of residual thermal stresses could be carried out by adding an extra term to the mechanical strain. The comparison with experiments shows a clear relevance of the residual stresses on the final strength of the inner ply. In fact, all the theoretical models highly overestimates the strength when they are implemented without residual thermal stresses.

The post-mortem observation of the laminates shows a very different behavior for thick and thin laminates. Whereas thick laminates present a progressive increase of transverse cracks, the thinnest laminates develop delamination immediately after the first transverse crack onsets or even before any transverse cracking. This observation suggests that the prediction for the thinnest laminates should combine the models for transverse

cracking along with models for other types of failure as free-edge delaminations, as that presented by Martin et al. (2010).

Finally, in order to compare different theoretical models, it would be necessary new experiments allowing to observe the validity of their very different hypotheses. Such an analysis would require micromechanical models and experiments since the majority of these models are based on hypotheses about the failure behavior at the microscale.

7. Acknowledgements

Experimental tests presented were carried out by A. Simon during her student fellowship at the University of Seville under the program Erasmus in 2013. The authors are indebted to Professors Federico París and Antonio Blázquez (University of Seville) for inspiring discussions, and to the latter also for his BEM code used in $\hat{G}$ calculation. The authors wish to thank the Spanish Ministry of Economy and Competitiveness and European Regional Development Fund (Projects MAT2012-37387 and MAT2015-71036-P, MINECO/FEDER, UE) for supporting this research.

Appendix A. Detail of experimental results

The results obtained from the experiments carried out in the Laboratory of the Group of Elasticity and Strength of Materials of the University of Seville are detailed in Table A.2.

n_{90°	specimen	$2t_{90}$ (mm)	$\varepsilon_{yy}^{c1}(\%)$	$\varepsilon_{yy}^{c2}(\%)$
1	1-1	0.201	0.6766	-
1	1-2	0.164	0.6684	-
1	1-3	0.193	0.5276	-
1	1-4	0.180	1.0872	-
1	1-5	0.197	0.5302	-
2	2-1	0.357	0.5436	0.5436
2	2-2	0.380	0.2698	0.5892
2	2-3	0.386	0.4040	0.6296
2	2-4	0.372	0.4846	0.6430
2	2-5	0.359	0.3946	0.4994
2	2-6	0.395	0.2900	0.5074
3	3-1	0.570	0.3798	0.3932
3	3-2	0.591	0.2846	0.3530
3	3-3	0.573	0.3772	0.3932
3	3-4	0.588	0.2550	0.3678
3	3-5	0.584	0.3920	0.4590
3	3-6	0.573	0.1584	0.2926
4	4-1	0.761	0.2778	0.3248
4	4-2	0.762	0.2684	0.3194
4	4-3	0.794	0.2832	0.3088
4	4-4	0.801	0.3356	0.4590
4	4-5	0.788	0.4188	0.4188
4	4-6	0.763	0.4524	0.4818
5	5-1	0.940	0.2966	0.3074
5	5-2	0.985	0.1838	0.1838
5	5-3	0.925	0.2174	0.2174
5	5-4	0.942	0.2120	0.2940
5	5-5	0.929	0.2134	0.2496
5	5-6	0.961	0.1558	0.2108
7	7-1	1.375	0.2202	0.2672
7	7-2	1.395	0.1598	0.2564
7	7-3	1.369	0.1692	0.2308
7	7-4	1.339	0.1046	-
7	7-5	1.346	0.1262	0.2322
7	7-6	1.329	0.1664	0.1852
10	10-1	1.899	0.2000	-
10	10-2	1.915	0.1422	0.3046
10	10-3	1.937	0.1276	0.2214
10	10-4	1.923	0.1100	0.2604
10	10-5	2.002	0.1168	0.3194
10	10-6	1.97	0.1974	-
16	16-1	2.892	0.1424	-
16	16-2	2.988	0.2336	0.3300
16	16-3	3.001	0.1960	0.2040
16	16-4	2.886	0.2228	-
16	16-5	2.847	0.1960	-

Table A.2: Experimental results obtained for the new set of tests of geometrically similar laminates of carbon/epoxy AS4/8852 with $t_0/t_{90} = 2$.

Appendix B. Computation of the energy release rate G

The energy release rate G is extracted in its dimensionless form as $\hat{G}$, defined in (5), using a Boundary Element Method (BEM) code by Blázquez et al. (2008). Based on the results of this BEM code a function for $\hat{G}$ was generated using a quadratic spline interpolation. The results are detailed in Figure B.8.

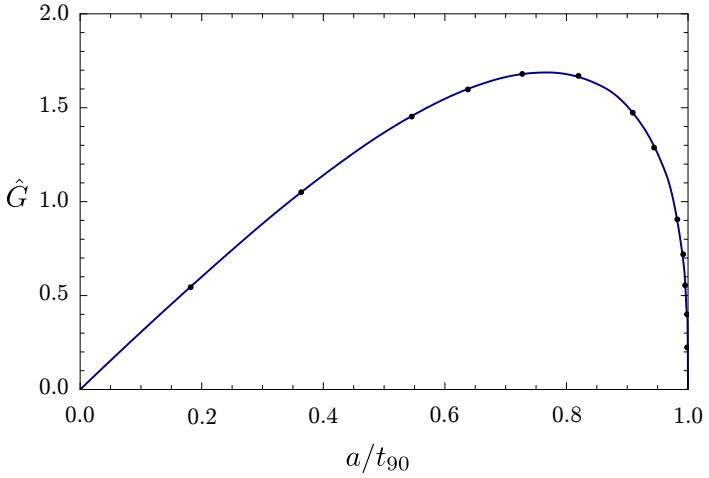

a/t_{90}	$\hat{G}$
0.000000	0.000000
0.181818	0.547499
0.363636	1.05027
0.545455	1.45584
0.636364	1.59838
0.727273	1.67914
0.818182	1.66534
0.909091	1.47369
0.945455	1.28699
0.981818	0.907757
0.990909	0.715565
0.995455	0.558484
0.998182	0.401307
0.999636	0.223171
1.000000	0.000000

Figure B.8: Results of the dimensionless energy release rate $\hat{G}$ used for the implementation of the theoretical models.

References

ASTM Standard D3039 (2006). Standard test method for tensile properties of polymer matrix composite materials. West Conshohocken, PA: ASTM International.

ASTM Standard D3518 (2007). Standard test method for in-plane shear response of polymer matrix composite materials by tensile test of a ±45° laminate. West Conshohocken, PA: ASTM International.

Aveston, J., G. A. Cooper, and A. Kelly (1971). The properties of fiber composites. In *Conference Proceeding. National Physical Laboratory, Guildford*, Teddington, pp. 15–26. IPC Science and Technology Press.

Berthelot, J. (2003). Transverse cracking and delamination in cross-ply glass-fiber and carbon-fiber reinforced plastic laminates: Static and fatigue loading. *Applied Mechanics Reviews 56*(1), 111–147.

Blázquez, A., V. Mantič, F. París, and L. McCartney (2008). Stress state characterization of delamination cracks in [0/90] symmetric laminates by BEM. *International Journal of Solids and Structures 45*(6), 1632–1662.

Boniface, L., P. A. Smith, and M. G. Bader (1997). Transverse Ply Cracking in Cross-Ply CFRP LaminatesInitiation or Propagation Controlled? *Journal of Composite Materials*, 1080–1112.

Camanho, P. P., C. G. Dávila, S. T. Pinho, L. Iannucci, and P. Robinson (2006). Prediction of in situ strengths and matrix cracking in composites under transverse tension and in-plane shear. *Composites Part A: Applied Science and Manufacturing 37*(2), 165–176.

Chang, F.-K. and M.-H. Chen (1987). The In Situ Ply Shear Strength Distributions in Graphite/Epoxy Laminated Composites. *Journal of Composite Materials 21*(8), 708–733.

Dvorak, G. J. and N. Laws (1985). Mechanics of first ply failure in composite laminates. *American Society of Mechanical Engineers, Applied Mechanics Division 74*, 59–69.

Dvorak, G. J. and N. Laws (1986). Analysis of first ply failure in composite laminates. *Engineering Fracture Mechanics 25*(5-6), 763–770.

Dvorak, G. J. and N. Laws (1987). Analysis of progressive matrix cracking in composite laminates - II. First ply failure. *Journal of Composite Materials 21*(4), 309–329.

Flaggs, D. L. and M. H. Kural (1982). Experimental Determination of the In Situ Transverse Lamina Strength in Graphite/Epoxy Laminates. *Journal of Composite Materials 16*(2), 103–116.

García, I. G. (2014). *Crack initiation in composites at micro and meso scales: Development and applications of finite fracture mechanics*. Ph. D. thesis, School of Engineering, University of Seville.

García, I. G., B. J. Carter, A. R. Ingraffea, and V. Mantič (2016). A numerical study of transverse cracking in cross-ply laminates by 3D finite fracture mechanics. *Composites Part B: Engineering 95*, 475–487.

García, I. G., V. Mantič, A. Blázquez, and F. París (2014). Transverse crack onset and growth in cross-ply [0/90]s laminates under tension. Application of a coupled stress and energy criterion. *International Journal of Solids and Structures 51*(23-24), 3844–3856.

García, I. G., V. Mantič, and A. Blázquez (2018). The effect of residual thermal stresses on transverse cracking in cross-ply laminates. An application of the Coupled Criterion of the Finite Fracture Mechanics. *International Journal of Fracture 211*, 61–74.

Garrett, K. W. and J. E. Bailey (1977). Multiple transverse fracture in 90° cross-ply laminates of a glass fibre-reinforced polyester. *Journal of Materials Science 12*(1), 157–168.

Hashin, Z. (1996). Finite thermoelastic fracture criterion with application to laminate cracking analysis. *Journal of the Mechanics and Physics of Solids 44*(7), 1129–1145.

Hinton, M. J. and A. S. Kaddour (2013). The background to Part B of the Second World-Wide Failure Exercise: Evaluation of

theories for predicting failure in polymer composite laminates under three-dimensional states of stress. *Journal of Composite Materials 47*, 643–652.

Hinton, M. J., A. S. Kaddour, and P. D. Soden (2004). *Failure criteria in fibre reinforced polymer composites: The World-Wide Failure Exercise*. Oxford: Elsevier.

Ho, S. and Z. Suo (1993). Tunneling Cracks in Constrained Layers. *Journal of Applied Mechanics 60*(4), 890.

ISO Standard 15024 (2001). Fibre-reinforced plastic composites - Determination of mode I interlaminar fracure toughness, G1C, for unidirectionally reinforced materials. Geneva, Switzerland: ISO.

Jalalvand, M., M. R. Wisnom, H. Hosseini-toudeshky, and B. Mohammadi (2014). Experimental and numerical study of oblique transverse cracking in cross-ply laminates under tension. *Composites Part A 67*, 140–148.

Landis, C. M., I. J. Beyerlein, and R. M. McMeeking (2000). Micromechanical simulation of the failure of fiber reinforced composites. *48*(3), 621–648.

Leguillon, D. (2002). Strength or toughness? A criterion for crack onset at a notch. *European Journal of Mechanics and Solids 21*(1), 61–72.

Li, D. S. and M. R. Wisnom (1997). Evaluating Weibull parameters for transverse cracking in cross-ply laminates. *Journal of Composite Materials 31*(9), 935–951.

Maimí, P., P. P. Camanho, J. A. Mayugo, and C. G. Dávila (2007). A continuum damage model for composite laminates: Part I - constitutive model. *Mechanics of materials 39*, 897–908.

Manders, P., T. Chou, F. Jones, and J. Rock (1983). Statistical analysis of multiple fracture in 0/90/0 glass fibre/epoxy resin laminates. *Journal of Materials Science 18*(10), 2876–2889.

Marlett, K. (2010). Hexcel 8852 AS4 unidirectional prepreg at 190 gsm & 35% RC qualification material property data report. Technical Report CAM-RP-2010-002 Rev A, National Institute for Aviation Research. Wichita State University, Wichita, Kansas.

Martin, E., D. Leguillon, and N. Carrère (2010). A twofold strength and toughness criterion for the onset of free-edge shear delamination in angle-ply laminates. *International Journal of Solids and Structures 47*(9), 1297–1305.

Nairn, J. A. (2000). Matrix microcracking in composites. In A. Kelly and C. Zweben (Eds.), *Comprehensive Composite Materials*, Volume 2, pp. 403–432. Oxford: Pergamon.

Nouri, H., G. Lubineau, and D. Traudes (2013). An experimental investigation of the effect of shear-induced diffuse damage on transverse cracking in carbon-fiber reinforced laminates. *Composite Structures 106*, 529–536.

Okabe, T., H. Imamura, Y. Sato, R. Higuchi, J. Koyanagi, and R. Talreja (2015). Experimental and numerical studies of initial cracking in CFRP cross-ply laminates. *68*, 81–89.

Okabe, T., H. Sekine, J. Noda, M. Nishikawa, and N. Takeda (2004). Characterization of tensile damage and strength in GFRP cross-ply laminates. *Materials Science and Engineering: A 383*(2), 381–389.

París, F. (2001). A study of failure criteria of fibrous composite materials. Technical report, NASA CR-2001-210661.

París, F., A. Blázquez, L. McCartney, and A. Barroso (2010b). Characterization and evolution of matrix and interface related damage in [0/90]s laminates under tension. Part II: Experimental evidence. *Composites Science and Technology 70*(7), 1176–1183.

París, F., A. Blázquez, L. McCartney, and V. Mantič (2010a). Characterization and evolution of matrix and interface related damage in [0/90]s laminates under tension. Part I: Numerical predictions. *Composites Science and Technology 70*(7), 1168–1175.

París, F., E. Correa, and J. Cañas (2003). Micromechanical view of failure of the matrix in fibrous composite materials. *Composites Science and Technology 63*(7), 1041–1052.

Parvizi, A. and J. Bailey (1978). On multiple transverse cracking in glass fibre epoxy cross-ply laminates. *Journal of Materials Science 13*(10), 2131–2136.

Parvizi, A., K. Garrett, and J. Bailey (1978). Constrained cracking in glass fibre-reinforced epoxy cross-ply laminates. *Journal of Materials Science 13*(1), 195–201.

Renart, J., N. Blanco, E. Pajares, J. Costa, S. Lazcano, and G. Santacruz (2011). Side clamped beam (SCB) hinge system for delamination tests in beam-type composite specimens. *Composites Science and Technology 71*, 1023–1029.

Schultheisz, C. R. and A. M. Waas (1996). Compressive failure of composites, Part I: Testing and micromechanical theories. *32*(1), 1–42.

Smith, P. A., L. Boniface, and N. F. C. Glass (1998). A comparison of transverse cracking phenomena in (0/90)s and (90/0)s CFRP laminates. *Applied Composite Materials 5*(1), 11–23.

Soden, P. D., M. J. Hinton, and A. S. Kaddour (1998). A comparison of the predictive capabilities of current failure theories for composite laminates. *Composites Science and Technology 58*(7), 1225–1254.

Sun, C. T., B. J. Quinn, J. Tao, D. W. Oplinger, and W. J. Hughes (1996). Comparative evaluation of failure analysis methods for composite laminates. Technical report, DOT/FAA/AR-95/109.

Takeda, N. and S. Ogihara (1994). In situ observation and probabilistic prediction of microscopic failure processes in CFRP cross-ply laminates. *Composites Science and Technology 52*(2), 183–195.

Tay, T. E., G. Liu, V. B. C. Tan, X. S. Sun, and D. C. Pham (2008). Progressive failure analysis of composites. *42*(18), 1921–1966.

Tessema, A., S. Ravindran, and A. Kidane (2018). Gradual damage evolution and propagation in quasi-isotropic CFRC under quasi-static loading. *Composite Structures 185*, 186–192.

Tiryakioğlu, M. (2008). On estimating Weibull modulus by moments and maximum likelihood methods. *Journal of Materials Science 43*(2), 793–798.

van der Meer, F. P. and C. G. Dávila (2013). Cohesive modeling of transverse cracking in laminates under in-plane loading with a single layer of elements per ply. *International Journal of Solids and Structures 50*(20-21), 3308–3318.

Vasil'ev, V., A. Dudchenko, and A. Elpatévskii (1970). Analysis of the tensile deformation of glass-reinforced plastics. *Polymer Mechanics* (1), 127–130.

Wang, A. and F. Crossman (1980). Initiation and Growth of Transverse Cracks and Edge Delamination in Composite Laminates. Part 1. An Energy Method. *Journal of Composite Materials 14*, 71–87.

Wang, A. S. D. (1984). Fracture mechanics of sublaminate cracks in composite materials. *Composites Technology Review 6*(2), 45–62.

Wang, A. S. D., N. N. Kishore, and C. A. Li (1985). Crack development in graphite-epoxy cross-ply laminates under uniaxial tension. *Composites Science and Technology 24*, 1–31.
Weibull, W. (1939). The phenomenon of rupture in solids. *Ingeniors Vetankaps Akademien-Handlinger* (153).
Weißgraeber, P., D. Leguillon, and W. Becker (2016). A review of Finite Fracture Mechanics: crack initiation at singular and non-singular stress raisers. *Archive of Applied Mechanics 86*(1), 375–401.
Wevers, M. and M. Surgeon (2000). Acoustic emission and composites. In A. Kelly and C. Zweben (Eds.), *Comprehensive Composite Materials*, pp. 345–357. Oxford: Pergamon.